Available online at www.sciencedirect.com
SCIENCE DIRECT®
Journal of Solid State Chemistry 179 (2006) 389–397
JOURNAL OF SOLID STATE CHEMISTRY
www.elsevier.com/locate/jssc

Layered hybrid organic–inorganic Co(II) alkylphosphonates. Synthesis, crystal structure and magnetism of the first two members of the series: $Co[(CH_3PO_3)(H_2O)]$ and $Co[(C_2H_5PO_3)(H_2O)]$

Elvira M. Bauer[a], Carlo Bellitto[a,*], Marcello Colapietro[b,**], Said A. Ibrahim[c], Mohamed R. Mahmoud[c], Gustavo Portalone[b], Guido Righini[a]

[a]*CNR-Istituto di Struttura della Materia, Sez.2, Via Salaria Km. 29.5, C.P.10, I-00016, Monterotondo Stazione, Roma, Italy*
[b]*Dipartimento di Chimica, Università di Roma "La Sapienza", p.le A. Moro 5, 00185 Roma, Italy*
[c]*Department of Chemistry, Faculty of Science, University of Assiut, Assiut, Egypt*

Received 27 September 2005; received in revised form 21 October 2005; accepted 23 October 2005
Available online 5 December 2005

Abstract

$Co[(CH_3PO_3)(H_2O)]$ (**1**) and $Co[(C_2H_5PO_3)(H_2O)]$ (**2**) were prepared by the hydrothermal method and isolated as blue-violet platelet crystals. They were characterized by X-ray diffraction, FT-IR, TGA-DSC techniques and their magnetic properties studied by a dc-SQUID magnetometer. Compound (**1**) shows an hybrid layered structure, made of alternating inorganic and organic layers along the *a*-direction of the unit cell. The inorganic layers contain Co(II) ions six-coordinated by five phosphonate oxygen atoms and one from the water molecule. These layers are separated by bi-layers of methyl groups and van der Waals contacts are established between them. In compound (**2**), the layered hybrid structure is rather similar to that described for compound (**1**), but the alternation of the inorganic and organic layers is along the *b*-direction of the unit cell. The magnetic behavior of (**1**) and (**2**) as function of temperature and magnetic field was studied. The compounds obey the Curie–Weiss law at temperatures above 100 K, the Curie C, and Weiss θ constants for the methyl derivative being $C = 3.36\,cm^3\,K\,mol^{-1}$ and $\theta = -53\,K$ and for the ethyl derivative $C = 3.62\,cm^3\,K\,mol^{-1}$ and $\theta = -75\,K$, respectively. The observed magnetic moments for Co atom at room temperature (i.e. $\mu_{eff} = 5.18$ and 5.38 BM, respectively) are higher than those expected for a spin-only value for high spin Co(II) ($S = 3/2$), revealing a substantial orbital contribution to the magnetic moment. The negative values of θ are an indication of the presence of antiferromagnetic exchange couplings between the near-neighbors Co(II) ions, within the layers. $[Co(C_nH_{2n+1}PO_3)(H_2O)]$ ($n = 1, 2$) are 2D Ising antiferromagnets at low temperatures.

Keywords: Cobalt(II) alkylphosphonates; Crystal engineering; Organic–inorganic hybrid materials; Magnetic properties

1. Introduction

Metal phosphonates are hybrid organic–inorganic materials in which the nature of the organic moiety can be designed to confer a specific property (intercalation, ionic exchange, proton conduction, catalysis, etc.) to the whole lattice. For this reason, the interest in the chemistry of phosphonates has drastically increased in the last 20 years [1]. Zr(IV) derivatives were the most studied metal-phosphonates and layered structures to the parent zirconium hydrogen phosphate were found. Later the studies were focused on metal(II) and metal(III) derivatives [2], and, more recently, the research has been addressed to the design and synthesis of new and multifunctional phosphonate ligands in an attempt to obtain new molecular and lattice architectures (see for example [3]). The unusual compositional and structural diversity of these materials through the most common layered frameworks [4–7] has stimulated extensive research on their chemistry.

An attractive feature of many metal(II) phosphonates is the two-dimensional character of the lattice, in which the

*Corresponding author. Fax: +39 0690672316.
**Also to be corresponded.
E-mail addresses: carlo.bellitto@ism.cnr.it (C. Bellitto), m.colapietro@caspur.it (M. Colapietro).

0022-4596/$ - see front matter © 2005 Elsevier Inc. All rights reserved.
doi:10.1016/j.jssc.2005.10.035

metal containing layers are separated each other by the organic sheets and alternate along one direction of the unit cell, thus giving rise to an hybrid organic–inorganic layered structure. This kind of network can also crystallize in more than one phase and a recent example is represented by Fe[(CH_3PO_3)(H_2O)], where two crystallographic forms were identified [8c]. In these divalent metal phosphonates, the inorganic layers contain often the metal ion in octahedral symmetry [8–10,12]. However, in the case of the polar Cr(II) ammonium ethylphosphonate chloride, the metal ion was found to be pentacoordinated to five oxygens, one of which from a water molecule [11]. The latter type of coordination has also been observed in the Cu(II) phosphonate analogues [13]. Co(II) phosphonates have been reported recently in literature [14–18], and they show a variety of molecular structures and of crystalline lattices. For example, the coexistence of tetrahedral [CoO_4] and octahedral [CoO_6] units have been observed in the same lattice in Co_2[($O_3P(CH_2)PO_3$) (H_2O)] [17b,18d].

We have found a lack of detailed information on the crystal structure and the magnetic properties of the first and the second member of the cobalt(II) alkylphosphonates [18].

The present work deals with the synthesis, the X-ray single-crystal structure determination and magnetic properties of the first two members of the Co(II) alkylphosphonates: i.e. Co[$CH_3PO_3(H_2O)$], (**1**), and of Co[(C_2H_5 PO_3)(H_2O)], (**2**).

2. Experimental section

2.1. Materials and methods

Methyl phosphonic acid (Aldrich), ethyl phosphonic acid (Aldrich) and urea (Carlo ERBA) were of analytical grade and were used without further purification. Co(II) chloride [$CoCl_2 \cdot 6H_2O$] and Co(II) carbonate, [$2CoCO_3 \cdot 3Co(OH)_2$, 48–53% Co], were used as supplied from Carlo Erba. HPLC water was used as a solvent.

2.2. Synthesis and crystal growth of Co[(CH_3PO_3)(H_2O)]

The synthesis of Co[(CH_3PO_3)(H_2O)] has been reported previously [18b]. A typical preparation for the synthesis of single-crystals suitable for X-ray investigation is reported below. Methylphosphonic acid (1.34 g, 16.75 mmol) was dissolved in 50 mL of HPLC water and added to an equimolar amount of basic Co(II) carbonate, [$2CoCO_3 \cdot 3Co(OH)_2$] (1.64 g, 13.35 mmol). The mixture was then placed in the Teflon-lined stainless steel autoclave that was sealed and kept at 190 °C for 3 days under autogenous pressure. A deep violet microcrystalline product was isolated, filtered, washed several times with water, then with methanol and finally dried to the air. *Anal.% calcd. for Co[(CH_3PO_3)(H_2O)]: C, 7.03; H, 2.95; found: C, 7.04; H, 2.75.*

2.3. Synthesis and crystal growth of Co[($C_2H_5PO_3$)(H_2O)]

The growth of a suitable single crystal of Co[(C_2H_5 PO_3)(H_2O)] for X-ray studies was carried out in a sealed ampoule and under an inert atmosphere. $CoCl_2 \cdot 6H_2O$ (1.18 g, 4.96 mmol), ethylphosphonic acid, $C_2H_5PO_3H_2$ (0.55 g, 5.00 mmol) and urea, NH_2CONH_2 (0.60 g, 23.97 mmol), were placed in a glass ampoule and degassed under vacuum. Degassed water (20 mL) was then added and the ampoule was sealed under a static vacuum. For safety reasons, the ampoule was inserted in a stainless steal tube, placed in a programmable oven and heated up to 90 °C. After a week the reaction mixture was left to cool slowly to room temperature and dark violet platelets were isolated, washed with water and dried to the air. The final pH of the aqueous reaction filtrate was found to be 6.7. *Anal. % calcd. for Co[($C_2H_5PO_3$)(H_2O)]: C, 12.99; H, 3.81; found: C, 12.82, H, 3.61.*

2.4. Characterization and physical measurements

Elemental analyses were made by the Servizio di Microanalisi della Area di Roma del CNR. Thermogravimetric (TGA) data were measured in flowing dry nitrogen at a heating rate of 10 °min^{-1} on a Stanton-Redcroft STA-781 thermoanalyzer. The FT-IR absorption spectra were recorded on a Perkin-Elmer 621 spectrophotometer using KBr pellets. Static magnetic susceptibility measurements were obtained by using a Quantum Design MPMS5 SQUID magnetometer in fields up to 5 T. A freshly prepared sample was filled in a cellulose capsule and placed inside a polyethylene straw at the end of the sample rod. All the experimental data were corrected for the core magnetization using Pascal's constants.

2.5. Structural characterization

X-ray powder diffraction analysis of Co[(CH_3PO_3 (H_2O)]. Room-temperature X-ray powder diffraction data were collected on a Seifert XRD-3000 diffractometer equipped with a curved graphite monochromator [λ (Cu$K\alpha_{1,2}$) = 1.54056/1.5444 Å] and a scintillation detector. The data were collected with a step size of 0.02°, $\Delta 2\theta$ and a counting time of 8 s per step over the range $4° < 2\theta < 80°$. The sample was mounted on a flat glass plate giving rise to a strong preferred orientation. The diffractometer zero point was determined from an external Si standard.

The X-ray powder diffraction patterns of the title compound was indexed using the TREOR program [19a] suggesting a primitive orthorhombic cell with the following unit cell parameters: $a = 17.39(1)$, $b = 4.79(1)$, $c = 5.65(1)$ Å. The fit is characterized by the figure of merit $M'(20) = 164$, $M(20) = 41$, and $F(20) = 51(0.0009, 42)$. The lattice parameters were found to be similar to those of one form of the layered Fe[$CH_3PO_3(H_2O)$], [8b] the unit

cell parameters and the space group of which is $Pna2_1$, suggesting for the cobalt(II) compound the same crystal structure of the latter. The structure was refined with the Rietveld method, by using a PC version of the crystal structure analysis package program GSAS [19b] with the graphical user interface EXPGUI [19c]. Powder diffraction patterns were calculated for this model in the orthorhombic space group $Pna2_1$, and by using the unit cell parameters obtained from X-ray crystal studies. Data were evaluated in the 7–75°, 2θ angular range (see Fig. S2). Using the utility *CONVX* [20], the raw data were transferred to the GSAS program package for full profile refinement. Initially the scale factor, the lattice parameters, the background coefficients and the peak shape were refined by the Le Bail method [21].

2.6. X-ray single-crystal studies of $Co[(CH_3PO_3)(H_2O)]$ and $Co[(C_2H_5PO_3)(H_2O)]$

The single crystals used for X-ray diffraction studies were violet platelets with dimensions approximately $0.1 \times 0.1 \times 0.1$ and $0.1 \times 0.1 \times 0.1$ mm, respectively. Details of the crystal data, data collection, structure solution, and refinements are reported in Table 1. Data were collected on a Huber CS diffractometer [22] with graphite monochromatized Mo$K\alpha$ radiation ($\lambda = 0.71069$ Å), using ω-scan. The crystals showed no decomposition during data collection. The data were corrected for *Lp* and for absorption, and the structures were solved by direct methods [23a] and refined anisotropically by full-matrix least-squares method. All the hydrogen atoms, with the exception of those belonging to the water molecule, were geometrically located and introduced into the final full-matrix least-squares refinement in a riding model with the isotropic temperature factors arbitrarily fixed. All final calculations were performed by SHELXL-97 and ORTEP-3 programs [23b,c]. The final residuals ($I > 2\sigma(I)$) were $R1 = 0.0297$ and w$R2 = 0.0855$, $R1 = 0.0466$ and w$R2 = 0.1251$ for compounds (**1**) and (**2**), respectively. Crystallographic data for the structures reported in this paper have been deposited with the Cambridge Crystallographic Data Center as supplementary publication no. CCDC 279766 for compound (**1**) and 255458 for compound (**2**). Copies of the data can be obtained free of charge on application to CCDC, 12 Union Road, Cambridge CB2 1EZ, UK (fax: (44) 1223 336-033; e-mail: deposit@ccdc.cam.ac.uk).

3. Results and discussion

3.1. Synthesis and structure

Cobalt(II) methylphosphonate was prepared by the hydrothermal reaction starting from basic cobalt(II)

Table 1
Crystallographic data and structure refinement for $Co[(CH_3PO_3)(H_2O)]$ and $Co[(C_2H_5PO_3)(H_2O)]$

(a) *Crystal data*		
Empirical formula	$Co[(CH_3PO_3)(H_2O)]$	$Co[(C_2H_5PO_3)(H_2O)]$
Formula weight ($g\,mol^{-1}$)	170.96	184.98
Temperature (K)	298	298
Crystal system	Orthorhombic	Monoclinic
Space group	$Pna2_1$	Pn
a (Å)	17.413(6)	4.806(2)
b (Å)	4.7856(3)	10.243(3)
c (Å)	5.6638(10)	5.674(1)
β (deg)		90.56(3)
V (Å^3)	471.99(18)	279.28(14)
D_c ($g\,cm^{-3}$)	2.406	2.176
Crystal size (mm^3)	$0.1 \times 0.05 \times 0.05$	$0.1 \times 0.1 \times 0.05$
Radiation (Å)	Mo$K\alpha$ (0.71069)	Mo$K\alpha$ (0.71069)
2θ range (deg)	4.29–34.99	3.98–39.97
h, k, l, collected	0–28, 0–7, 0–9	0–8, 0–18, ±10
Reflection collected	1301	1914
Unique reflection with $I \geqslant 2\sigma \mid I \mid$	847	1203
(b) *Structure solution and refinement*		
Refinement	$[F^2]$	$[F^2]$
Weighting scheme:	$w = 1/\sigma^2(F_o^2) + (0.0580P)^2 + 0.4189P$ with $P = (F_o^2 + 2F_c^2)/3$	$w = 1/\sigma^2(F_o^2) + (0.0816P)^2 + 0.8963P$ with $P = (F_o^2 + 2F_c^2)/3$
No. of params refined	64	78
$R(F^2)$	0.0297	0.0466
w$R(F^2)$	0.0855	0.1251
Goodness of fit	1.164	1.052

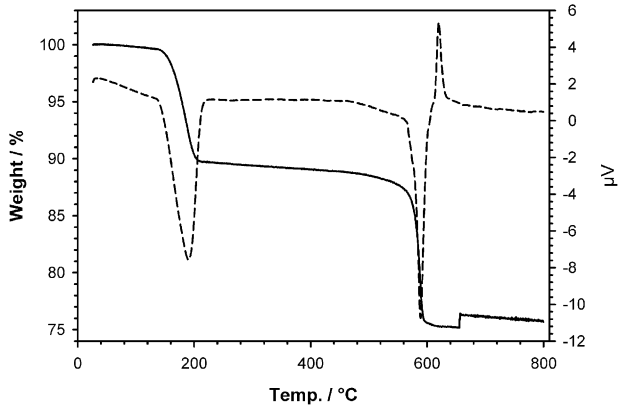

Fig. 1. TGA (————) and DSC (- - - - - - - -) of $Co[(C_2H_5PO_3)(H_2O)]$ (**2**).

carbonate with the appropriate phosphonic acid in water, and was isolated as a deep violet microcrystalline powder. A single-crystal of Co(II) ethylphosphonate suitable for X-ray studies was obtained from the reaction of $CoCl_2 \cdot 6H_2O$ with ethylphosphonic acid in a slightly modified synthetic procedure (see Section 2). The compounds were characterized by elemental analysis, TGA, XRD techniques as well as electronic and FT-IR spectroscopy. The TGA of compound (**1**) shows the first weight loss of 10.05% at $T = 217.7\,^{\circ}C$, and this process can be ascribed to the loss of one coordinated water molecule (the calculated value according to the above formula is 10.54%). In Co(II) ethylphosphonate, (see Fig. 1) the coordinated water is lost at $T = 201.7\,^{\circ}C$ and the experimental value of 9.76% is close to the calculated value for one water molecule, i.e. 9.74%. At higher temperatures a second weight loss corresponding to the decomposition of the organic part is observed.

3.2. $Co[(CH_3PO_3)(H_2O)]$ (*1*)

The title compound crystallizes in the orthorhombic space group $Pna2_1$, and its crystal structure has been solved from X-ray single-crystal studies. The crystallographic and experimental parameters of the title compound are reported in Table 1, selected bond distances and angles are reported in Table 2 and the ORTEP diagram is shown in Fig. 2. The unit cell packing of the title compound along the *c*-axis is shown in Fig. 3. The cobalt atoms are six-coordinated by five oxygens of the phosphonate groups, O(1), O(2), O(3), of different asymmetric units and one from the water molecule, O(w). Since the compound contains only one phosphonate per metal ion, all the phosphonate oxygen atoms take part in metal binding and two oxygens, O(1) and O(2), chelate the metal ion and, at the same time, bridge across adjacent metal-ions in the same row. Oxygens O(3) of the phosphonate lying in the mirror plane bonds to only one Co atom, and it is located *trans* to the oxygen O(w) of the water molecule. The $[CoO_6]$ octahedron is distorted and one of the *cis* O–Co–O angles, that subtended by the longer Co–O bond lengths, is small (~67°), while the others range between 84° and 96°. The

Table 2
Selected bond lengths (Å) and angles (deg) for non-H atoms for $Co[(CH_3PO_3)(H_2O)]$ with esd's in parentheses

$Co–O_1^a$	2.044(8)	$Co–O_1^b$	2.240(10)
$Co–O_2$	2.058(6)	$Co–O_2^b$	2.197(8)
$Co–O_3^c$	2.073(3)	$Co–O_w$	2.143(3)
P–C	1.787(4)	$P–O_1$	1.537(9)
$P–O_2$	1.564(7)	$P–O_3$	1.516(3)
$O_1^a–Co–O_w$	91.3(4)	$O_3^c–Co–O_w$	174.2(1)
$O_1^b–Co–O_w$	89.1(3)	$Co^d–O_1–Co^e$	121.0(5)
$O_1^b–Co–O_2$	103.0(1)	$Co–O_2–Co^e$	122.5(4)
$O_1^b–Co–O_2^b$	67.2(1)	$Co^d–O_1–P$	126.8(5)
$O_1^a–Co–O_2$	96.2(3)	$Co^e–O_2–P$	93.6(4)
$O_1^a–Co–O_2^b$	93.6(3)	$C–P–O_1$	105.6(7)
$O_1^a–Co–O_1^b$	160.8(4)	$C–P–O_2$	111.1(6)
$O_2–Co–O_2^b$	163.1(3)	$C–P–O_3$	109.1(2)
$O_2–Co–O_w$	91.9(3)	$O_1–P–O_2$	104.7(2)
$O_2^b–Co–O_w$	90.7(3)	$O_1–P–O_3$	113.0(6)
$O_1^a–Co–O_3^c$	91.6(4)	$O_2–P–O_3$	113.0(5)
$O_1^b–Co–O_3^c$	86.5(3)	$Co^d–O_3–P$	131.9(2)
$O_2–Co–O_3^c$	92.4(4)	$Co^e–O_1–P$	93.6(4)
$O_2^b–Co–O_3^c$	84.1(3)	$Co–O_2–P$	122.4(4)

[a] $x, y, z+1$.
[b] $-x+3/2, y+1/2, z+1/2$.
[c] $-x+3/2, y-1/2, z+1/2$.
[d] $x, y, z-1$.
[e] $-x+3/2, y-1/2, z-1/2$.

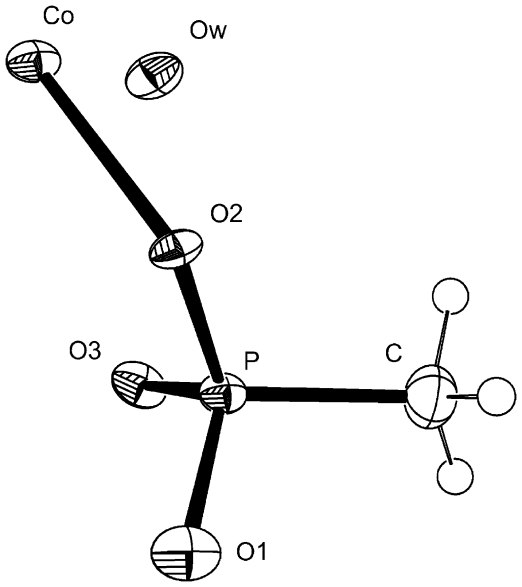

Fig. 2. ORTEP representation of the asymmetric unit of compound $Co[(CH_3PO_3)(H_2O)]$ (**1**).

Co–O distances in (**1**) range between 2.04(1) and 2.24(1) Å and are similar in value to those observed in other $[Co(II)O_6]$ octahedral compounds. The P–C bond (i.e. 1.79(1) Å) and the plane containing the methyl group are nearly perpendicular to the inorganic network (11° out of the perpendicular) and the orientation of the methyl group is disordered. Cobalt atoms are linked along the *b*-axis by the third oxygen of the phosphonate, O(2), to form a

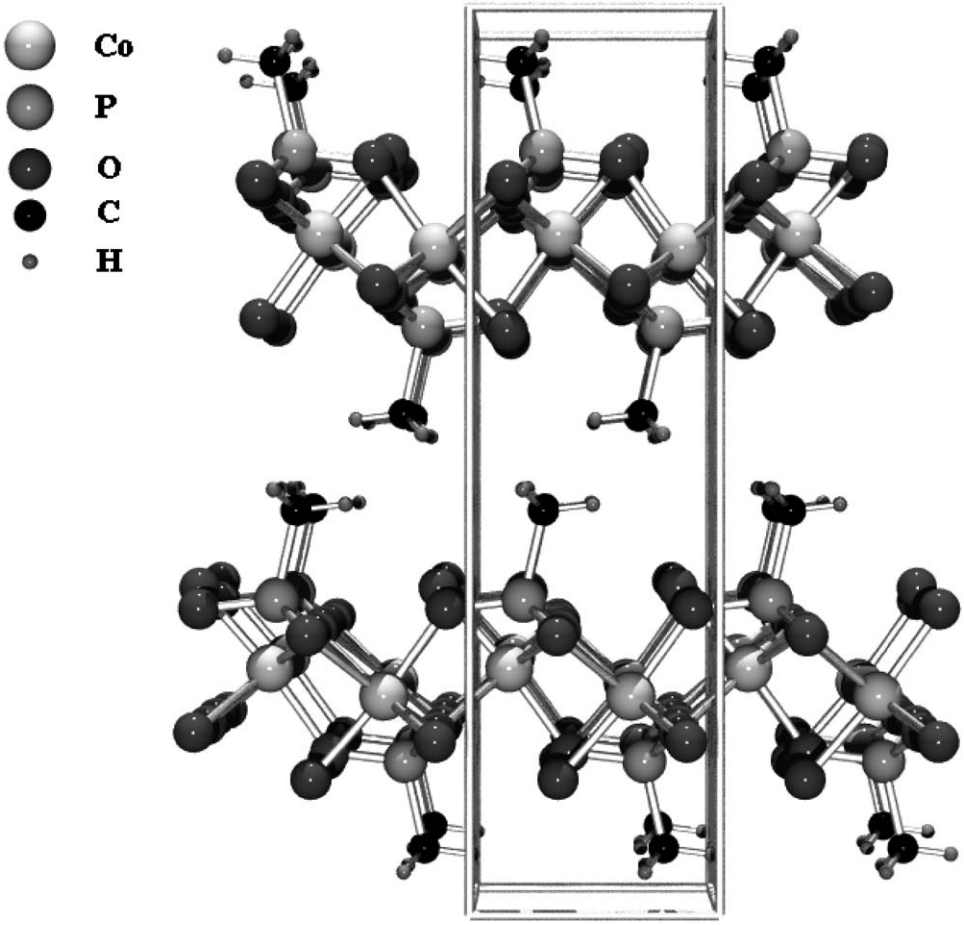

Fig. 3. Unit cell packing of $Co[(CH_3PO_3)(H_2O)]$ (**1**) viewed along the *b*-axis.

kinked or crenelated (*ac*) layer. The slabs of neutral $Co[(CH_3PO_3)(H_2O)]$ are then translationally related along the *a*-axis of the unit cell with only van der Waals contacts between them. The compound is isomorphous and isostructural with one form of $Fe[(CH_3PO_3)(H_2O)]$ [8b]. In order to check the presence of other phases in the $Co[(CH_3PO_3)(H_2O)]$ samples a X-ray powder diffraction study of the microcrystalline powder has been also performed (see Section 2). The Rietveld profile analysis, based on the structural model obtained from the X-ray crystal diffraction study has been carried out successfully, and it demonstrated that the sample used for magnetic studies and from which the single crystal has been picked up is a single phase and shows the same space group found in the single-crystal studied.

3.3. $Co[(C_2H_5PO_3)(H_2O)]$

Compound (**2**) crystallizes in a monoclinic space group *Pn*, and its crystal structure has been solved from X-ray single crystal studies. Crystallographic data and experimental parameters are reported in Table 1. Selected inter-atomic distances and bond angles of (**2**) are listed in Table 3 and the ORTEP diagram is shown in Fig. 4. The unit cell packing of (**2**) along the *c*-axis is shown in Fig. 5. The structure of inorganic layers is similar to that of the previous one with octahedral Co(II) ions coordinated by five oxygens of the phosphonate groups and one from the water molecule O(w). The octahedron $[CoO_6]$ is distorted and the lowest *cis* O–Co–O angle is 67.6(2)°, while the others range between 86.3(2)° and 96.8(2)°. The Co–O distances in (**2**) range between 2.062(4) and 2.248(5) Å being in the range of those observed in other $[CoO_6]$ octahedral compounds. The P–C bond is 1.790(6) Å and tilted by ca. 7° with respect to the *b* axis. The C–C bond of the ethyl group was found to be 1.536(11) Å. The layers are translationally related along the *b*-axis. $Co[(C_2H_5PO_3)(H_2O)]$ is isomorphous and isostructural with $Fe[(C_2H_5PO_3)(H_2O)]$ [10b]. A check of the structure of the microcrystalline powder of compound (**2**) performed by Rietveld analysis revealed the presence of a single phase, i.e. the structural identity of between the phase found from single-crystal study and that present in the powder used for the magnetic characterization.

3.4. Optical properties

Both the IR absorption spectra of $Co[(CH_3PO_3)(H_2O)]$ and $Co[(C_2H_5PO_3)(H_2O)]$ reveal features which can be rationalized on the basis of their molecular structure [9].

Table 3
Selected bond lengths (Å) and angles (deg) for non-H atoms for $Co[(C_2H_5PO_3)(H_2O)]$ with esd's in parentheses

$Co–O_1^a$	2.074(4)	$P–O_1$	1.559(4)
$Co–O_1^b$	2.159(4)	$P–O_2$	1.517(5)
$Co–O_2^c$	2.094(5)	$P–O_3$	1.554(4)
$Co–O_3$	2.062(4)	$P–C_1$	1.790(6)
$Co–O_3^b$	2.248(5)	$C1–C_2$	1.536(11)
$Co–O_w$	2.128(5)		
$O_1^a–Co–O_3$	102.3(2)	$O_1–P–O_2$	113.6(2)
$O_1^a–Co–O_3^b$	93.1(2)	$O_1–P–O_3$	104.0(2)
$O_1^a–Co–O_2^c$	90.3(2)	$O_1–P–C_1$	106.3(3)
$O_1^a–Co–O_w$	91.8(2)	$O_2–P–O_3$	113.2(2)
$O_1^a–Co–O_1^b$	160.7(2)	$O_2–P–C_1$	110.3(3)
$O_1^b–Co–O_3$	96.8(2)	$O_3–P–C_1$	108.9(3)
$O_1^b–Co–O_2^c$	86.3(2)	$Co^d–O_1–P$	123.9(2)
$O_1^b–Co–O_3^b$	67.6(2)	$Co^e–O_1–P$	95.8(2)
$O_1^b–Co–O_w$	90.0(2)	$Co^d–O_1–Co^e$	123.2(2)
$O_2^c–Co–O_3$	92.0(2)	$Co^e–O_2–P$	132.2(3)
$O_2^c–Co–O_w$	174.4(2)	$Co–O_3–P$	123.3(3)
$O_2^c–Co–O_3^b$	84.8(2)	$Co^e–O_3–P$	92.5(2)
$O_3–Co–O_w$	92.7(2)	$Co^e–O_3–Co$	121.3(2)
$O_3–Co–O_3^b$	164.2(2)	$C_2–C_1–P$	114.7(2)
$O_3^c–Co–O_w$	89.9(2)		

[a] $x, y, z+1$.
[b] $x-1/2, -y, z+1/2$.
[c] $x+1/2, -y, z+1/2$.
[d] $x, y, z-1$.
[e] $x+1/2, y, z-1/2$.

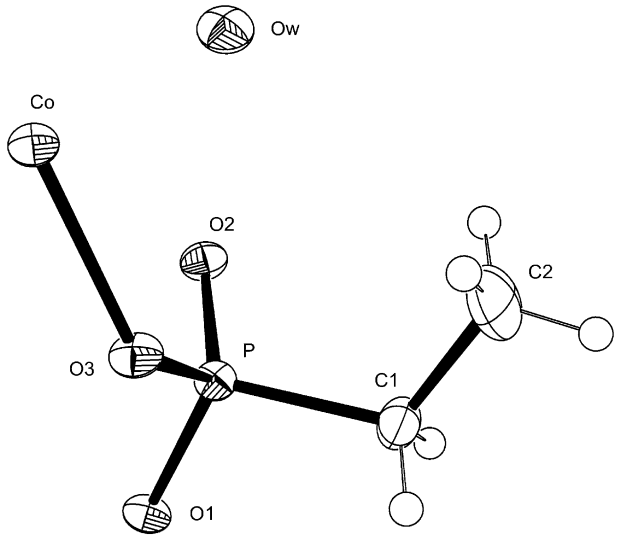

Fig. 4. ORTEP representation of the asymmetric unit of the crystal structure of compound $Co[(C_2H_5PO_3)(H_2O)]$ (**2**).

Typically, the FT-IR spectrum of (**2**) is reported in Fig. 6. It features two intense and sharp bands at 3420 and 3470 cm^{-1}, assigned to the OH stretching vibrations of coordinated water molecules. The band observed at 1610 cm^{-1} is assigned to the H_2O bending vibration. Two intense bands due to $[-PO_3]$ group vibrations are observed in the range 1200–970 cm^{-1}. Further, the complete deprotonation of the phosphonic acids in its Co(II) compounds is confirmed by the absence of the OH stretching vibration of P–OH at 2700–2550 and 2350–2100 cm^{-1}. Weak absorptions were observed in the range 2970–2924 cm^{-1} due to CH stretching vibrations of the methyl and ethyl groups.

The reflectance electronic spectra of the two compounds have also been measured. In the NIR-visible region composite bands with maxima centered at 542–546 and 731–743 nm have been observed. These bands are expected for Co(II) ions in a distorted octahedral stereochemical configuration and they can be assigned to the $^4T_{1g} \rightarrow {}^4T_{1g}(P)$ and $^4T_{1g} \rightarrow {}^4A_{2g}$ transitions, respectively. In fact the ground state of a Co(II) high spin ion is ^4F, but the orbital degeneracy is removed in O_h symmetry yielding one ^4A and two ^4T levels, the lowest-lying state being a $^4T_{1g}$ [24].

3.5. Magnetic properties

3.5.1. $Co[(CH_3PO_3)(H_2O)]$

Static magnetic susceptibility measurements were made on the polycrystalline sample with an applied field of 200 Oe from 5 to 270 K using a SQUID magnetometer. The temperature dependence of the inverse molar magnetic susceptibility of compound (**1**) is reported in Fig. 7. Above $T = 140$ K, it obeys the Curie–Weiss law, the Curie constant, C, being 3.36 $cm^3\,K\,mol^{-1}$ and the value of the Weiss constant, $\theta = -53$ K. The effective magnetic moment of 5.18 μ_B, is in the range of values observed for several high-spin octahedral Co(II) ions and is much larger than the spin-only value, μ_{so}, expected for spin $S = 3/2$ (i.e. 3.87 μ_B; $\mu_{so} = [4(SS+1)]^{1/2}$). This is consistent with the presence of a significant orbital contribution to the magnetic moment at high temperatures. The latter arises from the ground state triplet $^4T_{1g}$ of Co(II) ions in a octahedral crystal field [24,25]. The negative value of Weiss constant, i.e. $\theta = -53$ K, indicates antiferromagnetic near-neighbors exchange interactions between the adjacent Co(II) ions within the layers and/or zero-field splitting effects [25]. The χ vs. temperature plot shows an increase of χ with decreasing temperature particularly below 50 K (see Fig. 7) until a maximum at $T = 6.3$ K is observed, and this is an indication of antiferromagnetic interactions between the magnetic centers in a two-dimensional (2D) magnetic lattice (expected on the basis of the layered structure). The magnetic behavior should take into account two synergic factors in these systems: (a) the contribution of the orbital angular momentum and (b) the inter-ionic magnetic coupling between the nearest-neighbors Co(II) ions within the inorganic layers. The former factor derives from the fact that the degeneracy of $^4T_{1g}$ ground state can be removed by the action of axial and rhombic distortions of the crystal field as well as by spin–orbit coupling. The overall effect produces six Kramers doublets and results in a doublet ground state. Now, because the same doublet energy level remains lowest in energy for all the applied field strength and because the energy difference between the two lowest-lying doublets is relatively large with respect

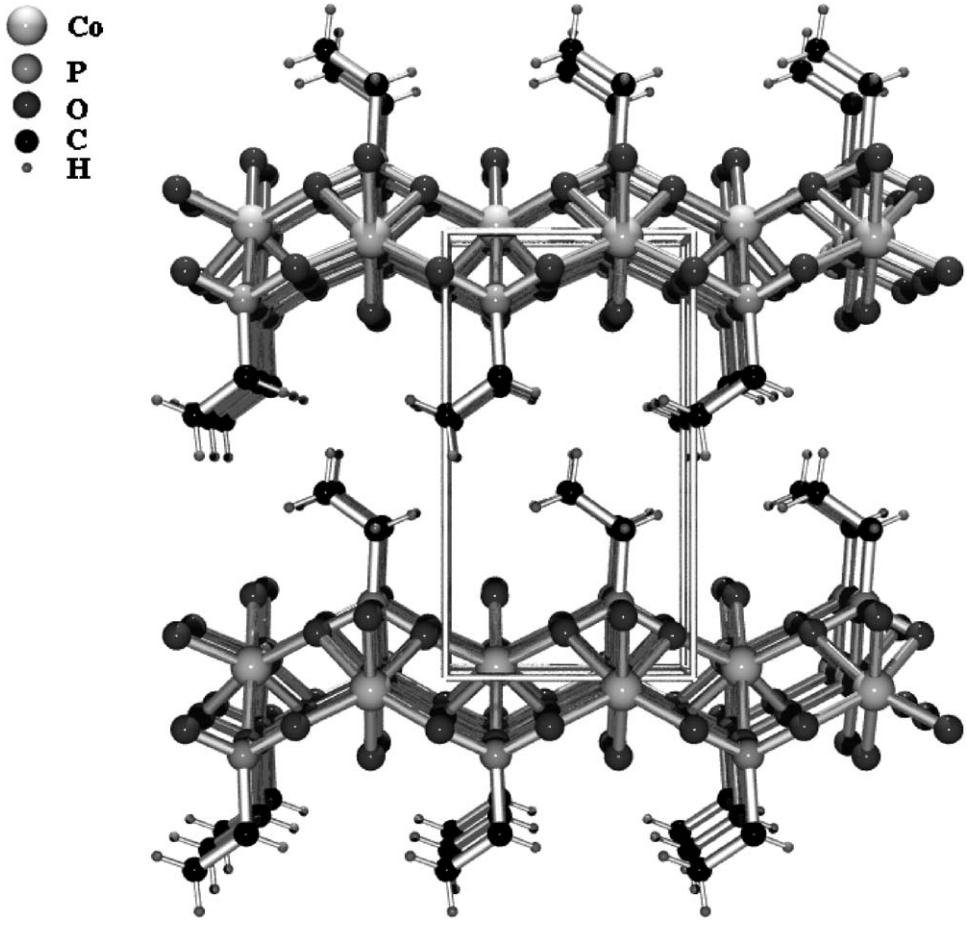

Fig. 5. Unit cell packing of Co[$(C_2H_5PO_3)(H_2O)$] (**2**) viewed along the *c*-axis.

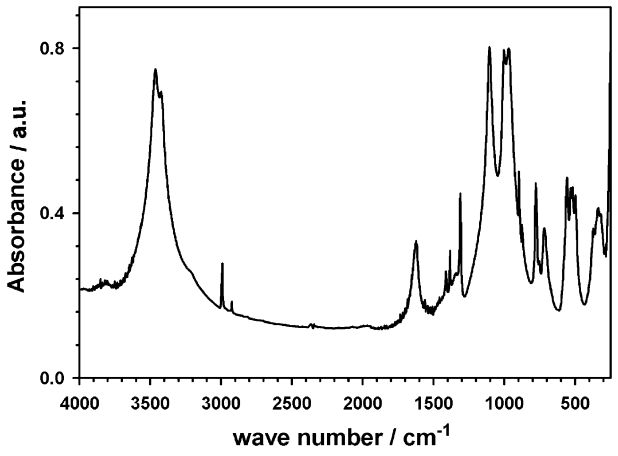

Fig. 6. Absorption FT-IR spectrum of Co[$(C_2H_5PO_3)(H_2O)$] **(2)** in the KBr region.

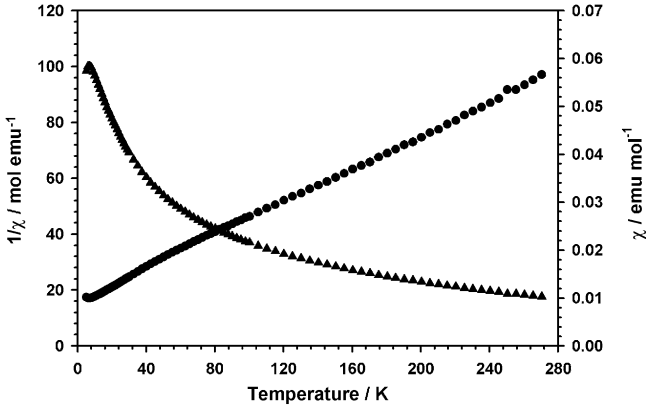

Fig. 7. $1/\chi$ vs. T plot (●) and χ vs. T plot (▲) for Co[$(CH_3PO_3)(H_2O)$] in the temperature range 5–270 K.

to the thermal energy present at low temperatures ($T<30$ K), the Co(II) ion can be described as having a ground state with an effective spin of $S=1/2$. The quantitative analysis of the magnetic properties for systems involving non isolated metal-ions with a significant orbital contribution is therefore a difficult task [26]. Attempts to reproduce the experimental magnetic susceptibility data vs. temperature, especially over the entire range of measured temperatures, by using the classical Heisenberg 2D square model and 2D Ising model were unsuccessful. The magnetization vs. field plot was also recorded at $T=5$ K, but it is not hysteretic and rules out the presence of ferromagnetic long-range ordering and in particular the presence of weak-ferromagnetism above 5 K.

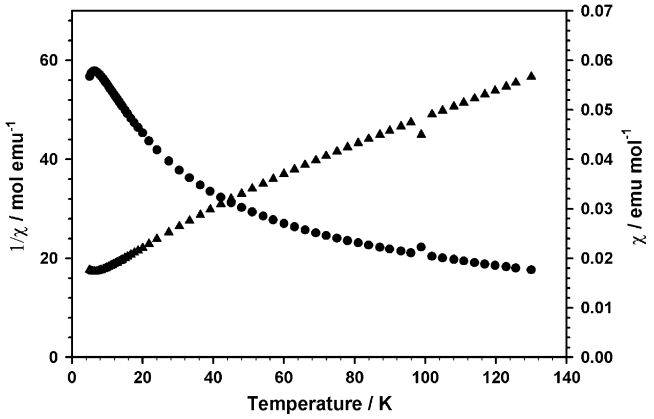

Fig. 8. Temperature dependence of $1/\chi$ vs. T (▲) and χ vs. T (●) for $Co[(C_2H_5PO_3)(H_2O)]$ in the temperature range 5–150 K.

3.5.2. $Co[(C_2H_5PO_3)(H_2O)]$

Static magnetic susceptibility measurements in both zero-field and field cooled modes were made on the polycrystalline sample of (**2**) with an applied field of 20 Oe in the temperature range 5–130 K using a SQUID magnetometer. There is a complete overlap between the two χ vs. T plots and the temperature dependence of the inverse molar magnetic susceptibility of compound (**2**) is reported in Fig. 8. Above $T = 60$ K, it obeys the Curie–Weiss law, the Curie constant being 3.62 $cm^3\,K\,mol^{-1}$ and the value of the Weiss constant, $\theta = -75$ K. The effective magnetic moment of 5.38 μ_B, is in the range of values observed for several high-spin octahedral Co(II) ions and is also in this case much larger than the spin-only value expected for spin $S = 3/2$ (i.e. 3.87 μ_B). The experimental magnetic data are similar to those reported for compound (**1**). On cooling a maximum is observed at $T = 6.5$ K in the χ vs. T plot, which also indicates in this compound the presence of antiferromagnetic interactions between the magnetic centers in a 2D magnetic lattice.

4. Conclusion

In this paper, we have reported the synthesis and the structural characterization of the first two members of Co(II) alkylphosphonates. Both Co(II) compounds show a layered hybrid organic–inorganic structure and they were found to be isomorphous and isostructural to the corresponding iron(II) alkylphosphonates. Cobalt(II) methylphosphonate reported in this work crystallizes in a space group different from that reported for the same compound by Mallouk, i.e. orthorhombic $Pna2_1$ [18b]. The result found by Mallouk was obtained from XRDP investigation and probably was not correct because of the low quality of the XRDP pattern used for the space group indexation or possibly due to the existence of more than one crystallographic form in $Co[(CH_3PO_3)(H_2O)]$, as observed recently in $Fe[(CH_3PO_3)(H_2O)]$ [8b,c]. This could be also the reason why difficulties were found in the past in solving the crystal structures of this class of materials by means of X-ray powder diffraction analysis with the Rietveld method. Another point which deserves a brief comment is the different magnetic behavior showed by the Fe(II) and Co(II) alkylphosphonates, although they have the same crystal structure and molecular structure. The former are weak-ferromagnets with a critical temperature, $T_N \sim 22$ K [8,10], while $Co[(C_6H_5PO_3)(H_2O)]$ [27] and the Co(II) compounds reported in this work are antiferromagnets (2D Ising type). The difference probably should be ascribed to the electronic ground state of Co(II) ions at very low temperatures. In the low-temperature region, the low-symmetry crystal field components together with spin–orbit coupling produce up to six Kramers doublets resulting in a doublet ground state ($S = 1/2$) which leads to anisotropic exchange coupling. Assuming that anisotropy is very strong, at low temperature the system can be considered as a 2D Ising system [25]. The weak-ferromagnetism in the Fe(II) phosphonates on the other hand has been rationalized on the basis of the Dzyaloshinsky–Moriya antisymmetric exchange mechanism [28]. Finally, it should be also noticed that there are in literature several Co(II) phosphonates, which are weak-ferromagnets, but their crystal and molecular structures are different [17c,18d,29].

Acknowledgments

This work is supported by MIUR-FIRB 2001 Program on ‘‘Ibridi organici-inorganici funzionali’’. The Consiglio Nazionale delle Ricerche (Italy) and the Academy of Scientific Research and Technology (Egypt) are also acknowledged for the financial support in the framework of their bilateral collaboration agreement.

Appendix A. Supplementary data

Supplementary data associated with this article can be found in the online version at doi:10.1016/j.jssc.2004.08.007.

References

[1] G. Alberti, in: J.-M. Lehn (Ed.), Comprehensive Supramolecular Chemistry, vol. 7, Pergamon Press, Oxford, 1996, pp. 151–185 and references therein.
[2] (a) D. Cunningham, P.J.D. Hennelly, T. Deeney, Inorg. Chim. Acta 37 (1979) 95
(b) A. Clearfield, in: K.D. Karlin (Ed.), Progress in Inorganic Chemistry, vol. 47, Wiley, New York, 1998, pp. 371–510;
(c) H.G. Harvey, B. Slater, M.P. Attfield, Chem. Eur. J. 10 (2004) 3270–3278;
(d) M. Riou-Cavellec, C. Serre, J. Robino, M. Nogues, J.-M. Greneche, G. Ferey, J. Solid. State Chem. 147 (1999) 122–131;
(e) A. Anillo, A. Altomare, A.G.G. Moliterni, E.M. Bauer, C. Bellitto, M. Colapietro, G. Portalone, G. Righini, J. Solid State Chem. 178 (2005) 306–313;
(f) C.A. Merryl, A.K. Cheetham, Inorg. Chem. 44 (2005) 5273–5277.
[3] (a) D. Kong, Y. Li, X. Ouyang, A.V. Prosvirin, H. Zhao, J.H. Ross, K.M. Dunbar, A. Clearfield, Chem. Mater. 16 (2004) 3020–3031;

(b) S.O.H. Gutschke, D.J. Price, A.K. Powell, P.T. Wood, Angew. Chem. Int. Ed. 38 (1999) 1088–1090.
[4] Z. Wang, A. Clearfield, J. Chem. Soc. Dalton Trans. (2002) 2937–2947.
[5] M.D. Poojary, H.L. Hu, F.L. Campbell III, A. Clearfield, Acta Crystallogr. Sect. B 49 (1993) 996–1001.
[6] (a) G. Cao, H. Lee, V.M. Lynch, T.E. Mallouk, Inorg. Chem. 27 (1988) 2781–2785;
(b) G. Cao, H. Lee, V.M. Lynch, J.S. Swinnea, T.E. Mallouk, Inorg. Chem. 29 (1990) 2112–2117;
(c) M.D. Poojary, B. Zhang, P. Bellinghausen, A. Clearfield, Inorg. Chem. 35 (1996) 4942–4949.
[7] A. Cabeza, M.A.G. Aranda, S. Bruque, M.D. Poojary, A. Clearfield, J. Sanz, Inorg. Chem. 27 (1998) 4168–4178.
[8] (a) A. Altomare, C. Bellitto, S.A. Ibrahim, M.R. Mahmoud, R. Rizzi, J. Chem. Soc. Dalton Trans. (2000) 3913–3919;
(b) C. Bellitto, F. Federici, M. Colapietro, G. Portalone, D. Caschera, Inorg. Chem. 41 (2002) 709–714;
(c) P. Léone, P. Palvadeau, K. Boubekeur, A. Meerschaut, C. Bellitto, E.M. Bauer, G. Righini, P. Fabritchnyi, J. Solid State Chem. 178 (2005) 1125–1132.
[9] (a) C. Bellitto, F. Federici, S.A. Ibrahim, Chem. Mater. 10 (1998) 1076–1082;
(b) C. Bellitto, F. Federici, S.A. Ibrahim, M.R. Mahmoud, 1998 MRS Fall Meetings Proceedings 547 (1999) 487–492;
(c) C. Bellitto, F. Federici, A. Altomare, R. Rizzi, S.A. Ibrahim, Inorg. Chem. 39 (2000) 1803–1808.
[10] (a) S.G. Carling, P. Day, D. Visser, R.K. Kremer, J. Solid State Chem. 106 (1993) 111–119;
(b) B. Bujoli, O. Pena, P. Palvadeau, J. le Bideau, C. Payen, J. Rouxel, Chem. Mater. 5 (1993) 583–587;
(c) C.T. Seip, G.E. Granorth, M.W. Meisel, D.R. Talham, J. Am. Chem. Soc. 119 (1997) 7084–7094.
[11] (a) E.M. Bauer, C. Bellitto, M. Colapietro, G. Portatone, G. Righini, Inorg. Chem. 43 (2003) 6345–6351;
(b) C. Bellitto, E.M. Bauer, G. Righini, A. Altomare, J. Magn. Magn. Mater. 272–276 (2004) 1060–1061.
[12] (a) E.M. Bauer, C. Bellitto, S.A. Ibrahim, M.R. Mahmoud, G. Righini, Chem. Eur. J. 9 (2003) 1324–1331;
(b) Q. Gao, N. Guillou, M. Nogues, A.K. Cheetham, G. Ferey, Chem. Mater. 11 (1999) 2937–2947.
[13] J.G. Mao, A. Clearfield, Inorg. Chem. 47 (2002) 2319–2324.
[14] H. Jankovics, M. Daskalakis, C.P. Raptopoulou, A. Terzis, V. Tangoulis, J. Giapintzakis, T. Kiss, A. Salifoglou, Inorg. Chem. 47 (2002) 3366–3374.
[15] A. Turner, P.A. Jaffers, E.J. MacLean, D. Villemin, V. McKee, G.B. Hix, J. Chem. Soc. Dalton Trans. (2003) 1314–1319.
[16] P. Yin, S. Gao, L.M. Zheng, Z. Wong, X.Q. Xin, Chem. Commun. 9 (2003) 1076–1077.
[17] (a) J. Le Bideau, A. Jounneaux, C. Payen, B. Bujoli, J. Mater. Chem. 4 (1994) 1319–1323;
(b) A. Distler, S.C. Sevov, Chem. Commun. (1998) 959–960;
(c) P. Rabu, P. Janvier, B. Bujoli, J. Mater. Chem. 9 (1999) 1323–1326.
[18] (a) G. Cao, H. Lee, V.M. Lynch, T.E. Mallouk, Inorg. Chem. 27 (1988) 2781–2785;
(b) G. Cao, T.E. Mallouk, Inorg. Chem. 30 (1991) 1434–1438;
(c) J. Le Bideau, C. Payen, B. Bujoli, P. Palvadeau, J. Magn. Magn. Mater. 140–144 (1995) 1719–1720;
(d) D.L. Lohse, S.C. Sevov, Angew. Chem. Int. Ed. 36 (1997) 1619–1621;
(e) A. Distler, D.L. Lohse, S.C. Sevov, J. Chem. Soc. Dalton Trans. (1999) 1805–1812;
(f) D. Cao, S. Gao, L.M. Zheng, J. Solid State Chem. 177 (2004) 2311–2315.
[19] (a) A. Altomare, C. Giacovazzo, A. Gagliardi, A.G.G. Moliterni, R. Rizzo, P.E. Werner, J. Appl. Crystallogr. 33 (2000) 1180–1186;
(b) A.C. Larson, R.B. Von Dreele, GSAS: Generalized Structure Analysis System, Report LAUR 86-748, Los Alamos National Laboratory, Los Alamos, NM, 1994;
(c) B.H. Toby, EXPGUI: a graphical user interface for GSAS, J. Appl. Cristallogr. 34 (2001) 210–213.
[20] For the program utility CONVX by M.E. Bowden see http://www.ccp14.ac.uk/
[21] A. Le-Bail, H. Duroy, J.L. Fourquet, Mater. Res. Bull. 23 (1988) 447–452.
[22] M. Colapietro, G. Cappuccio, C. Marciante, A. Pifferi, R. Spagna, J.R. Helliwell, J. Appl. Crystallogr. 25 (1992) 192.
[23] (a) A. Altomare, M.C. Burla, M. Camalli, G. Cascarano, C. Giacovazzo, A. Gagliardi, A.G.G. Moliterni, G. Polidori, R. Spagna, J. Appl. Crystallogr. 32 (1999) 115–119;
(b) G.M. Sheldrick, SHELXTL—97, Program for the Refinement of Crystal Structures, University of Göttingen, Germany, 1997;
(c) L.J. Farrugia, J. Appl. Crystallogr. 30 (1997) 565.
[24] B.N. Figgis, M.A. Hitchman, Ligand Field Theory and its Applications, Wiley-VCH, New York, 2000.
[25] O. Kahn, Molecular Magnetism, Wiley-VCH, New York, 1993.
[26] J.P. Garcia-Teran, O. Castello, A. Luque, U. Garcia-Courceiro, P. Roman, F. Loret, Inorg. Chem. 43 (2004) 5761–5770.
[27] J.F. Culp, G.E. Fanucci, B.C. Watson, A.N. Morgan, R. Bacov, H. Ohnuki, M.W. Meisel, D.R. Talham, J. Solid State Chem. 159 (2001) 362–370.
[28] (a) T. Moriya, Phys. Rev. 120 (1960) 91–98;
(b) I. Dzyaloshinsky, J. Phys. Chem. Solids 4 (1958) 241–255.
[29] (a) R. Adams, R. Layland, C. Payen, T. Datta, Inorg. Chem. 35 (1996) 3492–3497;
(b) P. Ying, X.-Q. Xin, S. Gao, L.M. Zheng, Inorg. Chem. 43 (2004) 2151–2156.